Roentgen Stereophotogrammetric Analysis Methods for Determining Ten Causes of Lengthening of a Soft-Tissue Anterior Cruciate Ligament Graft Construct

Conrad Smith
Biomedical Engineering Program,
University of California,
One Shields Avenue,
Davis, CA 95616

M. L. Hull[1]
Biomedical Engineering Program,
and Department of Mechanical Engineering,
University of California,
One Shields Avenue,
Davis, CA 95616
e-mail: mlhull@ucdavis.edu

S. M. Howell
Department of Mechanical Engineering,
University of California,
One Shields Avenue,
Davis, CA 95616

There are many causes of lengthening of an anterior cruciate ligament soft-tissue graft construct (i.e., graft + fixation devices + bone), which can lead to an increase in anterior laxity. These causes can be due to plastic deformation and/or an increase in elastic deformation. The purposes of this in vitro study were (1) to develop the methods to quantify eight causes (four elastic and four plastic) associated with the tibial and femoral fixations using Roentgen stereophotogrammetric analysis (RSA) and to demonstrate the usefulness of these methods, (2) to assess how well an empirical relationship between an increase in length of the graft construct and an increase in anterior laxity predicts two causes (one elastic and one plastic) associated with the graft midsubstance, and (3) to determine the increase in anterior tare laxity (i.e., laxity under the application of a 30 N anterior tare force) before the graft force reaches zero. Markers were injected into the tibia, femur, and graft in six cadaveric legs whose knees were reconstructed with single-loop tibialis grafts. To satisfy the first objective, legs were subjected to 1500 cycles at $\frac{1}{4}$ Hz of 150 N anterior force transmitted at the knee. Based on marker 3D coordinates, equations were developed for determining eight causes associated with the fixations. After 1500 load cycles, plastic deformation between the graft and WasherLoc tibial fixation was the greatest cause with an average of 0.8 ± 0.5 mm followed by plastic deformation between the graft and cross-pin-type femoral fixation with an average of 0.5 ± 0.1 mm. The elastic deformations between the graft and tibial fixation and between the graft and femoral fixation decreased averages of 0.3 ± 0.3 mm and 0.2 ± 0.1 mm, respectively. The remaining four causes associated with the fixations were close to 0. To satisfy the remaining two objectives, after cyclic loading, the graft was lengthened incrementally while the 30 N anterior tare laxity, 150 N anterior laxity, and graft tension were measured. The one plastic cause and one elastic cause associated with the graft midsubstance were predicted by the empirical relationships with random errors (i.e., precision) of 0.9 mm and 0.5 mm, respectively. The minimum increase in 30 N anterior tare laxity before the graft force reached zero was 5 mm. Hence, each of the eight causes of an increase in the 150 N anterior laxity associated with the fixations can be determined with RSA as long as the overall increase in the 30 N anterior tare laxity does not exceed 5 mm. However, predicting the two causes associated with the graft using empirical relationships is prone to large errors. [DOI: 10.1115/1.2904897]

Keywords: knee, anterior cruciate ligament graft, X-rays, laxity, lengthening, elongation

Introduction

Single-loop tibialis tendon allografts have increased in popularity owing to their many advantages over patellar tendon and double-loop hamstring tendon autografts for anterior cruciate ligament (ACL) reconstructions [1–5]. Nevertheless, clinically important increases in anterior laxity occur postoperatively in 9–22% of patients following ACL reconstruction for single-looped tibialis allografts [1,3]. Although the causes are unknown, increased anterior laxity can be traced to lengthening of the graft construct (i.e., graft-fixation-bone complex). To prevent clinically important increases in anterior laxity, it is of interest to determine the causes and corresponding amounts of lengthening of the graft construct because this information would be beneficial in devising measures to limit increases in anterior laxity.

Lengthening of the graft construct can be due to many causes, ten of which include plastic (i.e., nonrecoverable) deformations and increases in elastic deformations (Fig. 1). Plastic causes include plastic deformation (1) between femoral fixation and bone, (2) between the graft and femoral fixation, (3) between the graft and tibial fixation, (4) between the tibial fixation and bone, and (5) of the graft substance between the fixations. Elastic causes include an increase in elastic deformations due to a decrease in elastic stiffness (6) between the femoral fixation and bone, (7) between the graft and femoral fixation, (8) between the graft and tibial fixation, (9) between the tibial fixation and bone, and (10) of the graft substance between the fixations. Hence, eight of these ten causes are associated with the fixations (four plastic and four elastic) and two are associated with the graft (one plastic and one

[1]Corresponding author.

Contributed by the Bioengineering Division of ASME for publication in the JOURNAL OF BIOMECHANICAL ENGINEERING. Manuscript received January 16, 2007; final manuscript received September 19, 2007; published online May 16, 2008. Review conducted by Jeffrey A. Weiss.

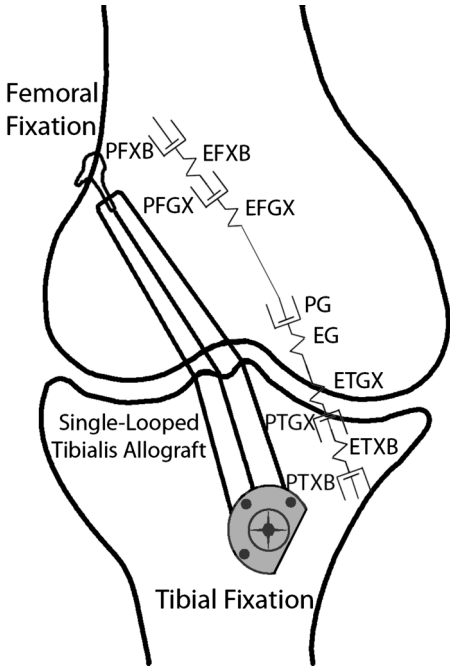

Fig. 1 Diagram depicting ten causes of lengthening of a soft-tissue ACL graft construct, which include five plastic causes and five elastic causes. The five plastic causes are nonrecoverable deformation (1) between the femoral fixation and bone (PFXB), (2) between the graft and femoral fixation (PFGX), (3) between the graft and tibial fixation (PTGX), (4) between the tibial fixation and bone (PTXB), and (5) of the graft substance between the fixations (PG). The five elastic causes are lengthening due to a decrease in elastic stiffness (1) between the femoral fixation and bone (EFXB), (2) between the graft and femoral fixation (EFGX), (3) between the graft and tibial fixation (ETGX), (4) between the tibial fixation and bone (ETXB), and (5) of the graft substance between the fixations (EG). Of these ten causes, the eight causes associated with the fixations were measured using RSA.

elastic). The various plastic causes lead to an increase in the slack (i.e., unloaded) length of the graft construct, whereas the various elastic causes lead to an additional increase in the length of the graft construct under load. Because some of these causes such as plastic lengthening of the graft midsubtance may result from biological processes (e.g., remodeling of the graft), these causes ultimately must be determined in vivo, which requires a proven method of measurement in vitro.

One method that offers the potential to directly quantify eight causes of lengthening associated with the fixations in vivo is Roentgen stereophotogrammetric analysis (RSA). RSA has been used previously to determine some of these causes [6–9] but to the knowledge of the authors, no study has demonstrated whether RSA can be used to quantify eight causes of lengthening of a graft construct associated with the fixations. Therefore, the first objective of this study was to develop the methods to determine these eight causes using RSA and to demonstrate the usefulness of these methods during cyclic loading of cadaveric knees.

Although the remaining two causes associated with the graft cannot be determined using RSA because the graft is not in a straight line, these two causes might still be determined by other means. If the eight causes associated with the fixations can be determined, then the deformations of the graft could be computed based on the relationships between graft construct lengthening and increases in anterior laxity. An empirical relationship between an increase in length of the graft construct and an increase in anterior laxity using an arthrometer has been determined previously [10,11]. However, to our knowledge, no previous study has determined an empirical relationship between an increase in length of the graft construct and an increase in anterior laxity using RSA. Therefore, the second objective was to determine an empirical relationship between lengthening of the graft construct and an increase in anterior knee laxity using RSA and assess whether this relationship can be used to predict the two causes associated with the graft.

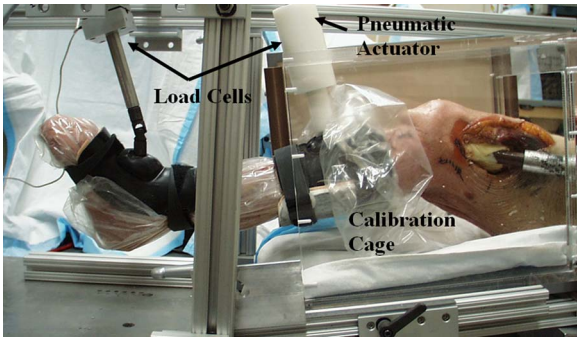

Fig. 2 Photograph of a cadaveric leg specimen in the loading apparatus. A pneumatic actuator applied either a posterior or anterior force to the tibia while the thigh and ankle were fixed with the specimen in a supine position and the knee was flexed to 25 degs. Two load cells measured the applied force and the reaction force at the ankle joint. The shear force transmitted at the knee was computed from the measured loads in conjunction with the weight of the specimen.

To differentiate between the elastic and plastic causes of an increase in anterior laxity, it is necessary to apply a small anterior tare force to the tibia to remove any slack in the graft. Under the application of a small tare force, the elastic deformations will be negligible so that only the plastic deformations will contribute to anterior displacement of the tibia with respect to the femur. If the tare force is not large enough to remove the slack, however, then any slack will become an error in the plastic deformations. Likewise, any slack not removed will become an error in elastic deformations, which are measured under the application of a relatively large anterior force (necessary to make elastic deformations measurable). It has been shown that graft force decreases after cyclic loading due to lengthening of the graft construct [12,13]. It is unknown how much lengthening due to plastic deformations of the graft construct can occur before the graft force reaches zero while an anterior tare force is applied to the tibia (i.e., the slack is not removed). The third objective of this study was to determine the increase in anterior tare laxity before the graft force reaches zero under an anterior tare force.

Methods

Experiments. Six cadaveric legs (average 69 years, range 53 to 87 years) were obtained and stored at −20°C. Radiographs and inspection of the knees at the time of ACL reconstruction did not reveal either moderate or severe degenerative arthritis, chondrocalcinosis, or torn menisci. The intact leg was thawed overnight before use. Four 0.8 mm diameter tantalum markers (Tilly Medical Products AB, Lund, Sweden) were implanted into both the femur and tibia.

A custom loading apparatus applied posterior and anterior forces to the proximal tibia of the leg specimens (Fig. 2). Forces perpendicular to the tibia at 12.5 cm distal to the joint line were applied by a pneumatic actuator, controlled to within ±1 N, and held within this range until simultaneous radiographs (described below) were taken (approximately 10–20 s). Three additional markers were fixed in a line along the pneumatic actuator to enable the identification of the loading axis from the radiographs.

To standardize the load transmitted at the knee joint line perpendicular to the tibia (referred to below as the *A-P shear force*

transmitted at the knee) and to increase the precision of the dependent variables computed using RSA [14], two load cells positioned in line with the attachment at the tibia and the attachment at the ankle were used. The weight of the shank-foot of each specimen was estimated using regression equations [15]. The sum of the two load cells was equal to the sum of the *A-P* shear force transmitted at the knee and the component of the weight perpendicular to the shank. Three *A-P* shear forces transmitted at the knee were standardized: a posterior force of 90 N, an anterior tare force of 30 N, and an anterior force of 150 N. This standardization ensured that the *A-P* shear force transmitted at the knee and particularly the 30 N anterior tare force were the same for each specimen independent of the weight of the specimen.

The RSA system included a calibration cage and two portable X-ray machines. The calibration cage (Tilly Medical Products AB, Lund, Sweden) contained markers at known positions to be used for system calibrations. The calibration cage was modified to hold two X-ray cassettes and two scatter grids (Medical X-Ray Enterprises, Inc., Culver City, CA) placed at right angles to each other (*A-P* and lateral views). The scatter grids were used to minimize exposure of the radiographic film from scattered X-rays and thus improve image quality. The calibration cage surrounded the tibiofemoral joint, such that all markers could be seen from each view. Each portable X-ray machine (Model HF80H+, MinXray Inc., Northbrook, IL) was positioned at a distance between 80 cm and 100 cm from its respective film plane so that the direction of X-rays was approximately orthogonal to this plane. The X-ray machine parameters were initially set to 15 mA at 0.1 s and 80 kV_p, and the exposure was adjusted by altering these parameters as needed depending on the bone density and thickness of the leg.

The legs were inserted into the loading apparatus and simultaneous radiographs were taken. The knees were flexed to 25 deg in the sagittal plane. This angle was defined between the lines extending along the femoral shaft and the tibial shaft using a goniometer. The line extending along the femoral shaft was defined between the center of the proximal end of the femoral shaft 20 cm proximal to the joint line and the lateral femoral epicondyle. The line extending along the tibial shaft was defined between the lateral femoral epicondyle and the lateral malleolus of the fibula. This flexion angle was selected because it is in the range where anterior knee laxity is the greatest [16]. Additionally, the tibia was placed in a position of neutral rotation, because this is the position of greatest laxity, in which all anterior force applied to the tibia is resisted by the ACL graft [16]. Simultaneous radiographs were taken in two planes (*A-P* view and lateral view) of the knee to define an anatomical coordinate system [14,17,18]. The leg was then preconditioned for 10 cycles between the 90 N posterior force and the 150 N anterior force. After preconditioning, simultaneous radiographs were taken as first the 90 N posterior force followed by the 150 N anterior force and were applied each for approximately 20 s.

Tibialis anterior and posterior tendon grafts were harvested from each leg. The midportion of each tendon was exposed and the skin and surrounding tendon sheath were cut exposing both the muscle and the distal insertion point of the tendon. The distal insertion point of the tendon was excised and the muscle was removed until the length of the tendon was a minimum 27 cm, at which point the proximal end was excised. The tendons were trimmed until they slid without resistance through a 9 mm sizing sleeve (Arthrotek, Inc., Warsaw, IN) when looped. To facilitate passing the graft around the cross-pin-type femoral fixation described below, 4 cm of the end of each strand were whip-stitched with a No. 1 braided, absorbable suture (Polysorb; United States Surgical/Syneture, Norwalk, CT) [19]. The tendons were then wrapped in a saline-soaked paper towel, and stored at −20°C.

The tibial metaphysis was reinforced with polyurethane foam to provide fixation structural properties in elderly cadaveric tibia similar to those in young human tibia [19]. The ACL was excised

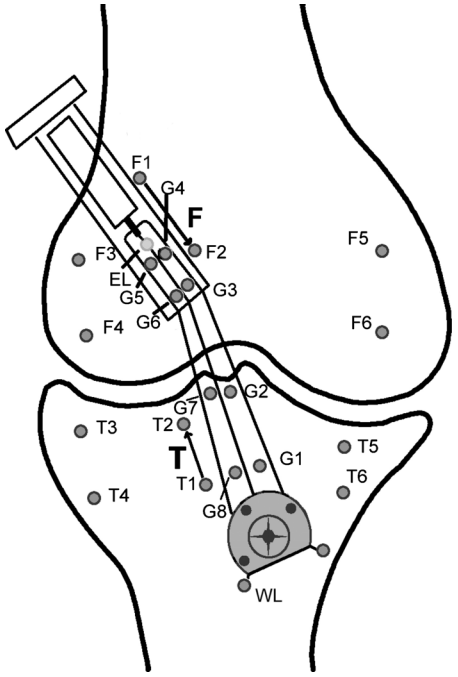

Fig. 3 *A-P* view of the knee showing marker placement. T1–T6 are markers implanted in the tibia, F1–F6 are markers implanted in the femur, G1–G8 are markers implanted in the graft, and EL and WL are markers attached to the femoral and tibial fixations, respectively. F and T are vectors aligned with the axes of the femoral and tibial tunnels, respectively.

and tibial and femoral drill holes were made using a previously described transtibial technique that positions the graft without roof impingement, without posterior cruciate ligament impingement, and with a tension pattern during passive flexion-extension that is similar to that of the intact ACL [20]. A tibial guide (Howell 65 deg Tibial Guide, Arthrotek Inc., Ontario, CA) was used to place a tibial tunnel so that the following criteria were met: (1) the tunnel axis was centered between the tibial spines and formed an angle of 65 ± 3 deg from the medial joint line of the tibia in the coronal plane, and (2) the tunnel was 5–6 mm posterior and parallel to the intercondylar roof at full extension in the sagittal plane. The tibial tunnel was drilled to the same diameter as the graft (i.e., 9 mm) using a tibial drill bit (Fully Fluted Cannulated Tibial Drills, Arthrotek, Inc.). A roof and wallplasty were performed to prevent impingement of the graft against the roof and wall of the intercondylar notch by inserting a metal rod, the same diameter as the tibial tunnel, so that it freely passed into the notch through the tibial tunnel with the knee in maximum hyperextension.

The femoral tunnel was positioned by inserting an over-the-top femoral aimer through the tibial tunnel (Size-Specific Femoral Aimer, Arthrotek, Inc.). An open-end femoral tunnel was drilled to 16 mm in diameter and a low-friction femoral bushing with an outer diameter of 16 mm and an inner diameter of 9 mm at its distal end was inserted into the femoral tunnel until flush with the intercondylar roof and fixed with bone cement [13]. This technique for placing the tibial and femoral tunnels endoscopically has good reproducibility between surgeons [21] and the tension pattern of the graft during passive flexion-extension is similar to that of the intact ACL [20].

To establish a vector that is parallel to the tunnel axes in each of the tibia and femur, two more markers were placed in the tibia and femur to establish tunnel vectors. Using a tunnel vector tool [22], two markers spaced 2 cm apart were inserted into the posterior wall of the tibial tunnel (T1 and T2, Fig. 3). The tunnel vector tool insured that the markers were inserted on a line that is parallel to

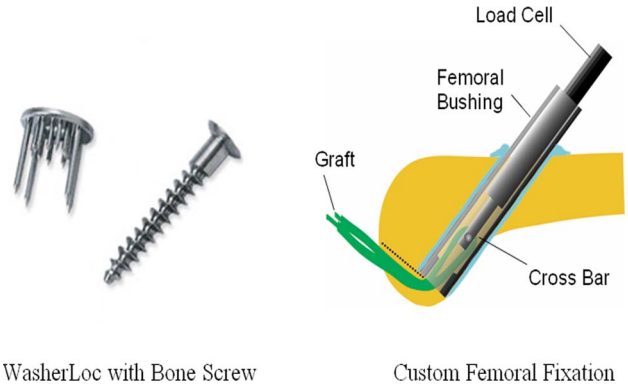

Fig. 4 Tibial (left) and femoral (right) fixation devices. The WasherLoc was used in our study as illustrated. A custom femoral fixation was used, which allowed the length of the graft construct to be adjusted and the graft tension to be measured [13]. The cross bar of the custom femoral fixation, around which the graft is looped, was similar in design to the EZLoc, a femoral fixation commonly used clinically. Also, like the custom femoral fixation, the EZLoc is supported by the cortical bone.

the axis of the tunnel. Two more markers were placed in the low-friction femoral bushing to establish the orientation of the femoral tunnel (F1 and F2, Fig. 3).

To quantify the motion of the fixation devices, titanium markers (Painful Pleasures, Owings Mills, MD) were welded to the WasherLoc (WL, Fig. 3) (WasherLoc, Arthrotek, Inc.) and to a custom femoral fixation device described in Ref. [13], which was used to simulate the EZLoc (EL, Fig. 3), a commonly used femoral fixation device (EZLoc, Arthrotek, Inc.). These markers were welded in locations such that upon insertion of the fixation devices into the respective bones, the fixation devices would not impede the view of the markers in the radiographs.

Radio-opaque tantalum markers were injected into each graft to quantify the various causes of lengthening of the graft construct. The graft was looped through the adjustable femoral fixation device with the thicker strand oriented medially until the strands were equal in length. The lengths of both tunnels and the intrarticular space were measured using a femoral tunnel depth gauge (Femoral Tunnel Depth Gauge, Arthrotek, Inc.). The portions of the graft contained within the femoral and tibial tunnels were marked onto the graft. Two 0.8 mm diameter markers (G1 and G5) were implanted into one strand and two 1.0 mm diameter markers (G4 and G8) were implanted into the other strand 5 mm proximal to the distal tibial tunnel mark and 5 mm distal to the proximal tibial tunnel mark (Fig. 3). Similarly, on the femoral side, two 0.8 mm markers (G2 and G6) were implanted into one strand and two 1.0 mm markers (G3 and G7) were implanted into the other strand 5 mm distal to the EL marker and 5 mm proximal to the distal femoral tunnel mark (Fig. 3). Markers were injected $\frac{3}{4}$ of the way through the diameter of the tendon with the injecting device perpendicular to the longitudinal axis of the tendon [23]. Using markers of different size allowed identification of each strand in the biplanar radiographs.

The graft was fixed in the femur using the custom femoral fixation, which allowed the length of the graft construct to be adjusted [13], and fixed in the tibia using the WasherLoc (Fig. 4). The distal ends of the graft were passed from proximal to distal through the low-friction femoral bushing, intrarticular space, and tibial tunnel. Tension was applied distally to the graft and the knee was flexed and extended for 15 cycles. With the knee in maximum extension, a 110 N load as measured using a load cell was applied to the distal end of the graft. This applied load was used because it restores the *A-P* laxity closely to normal [13]. The graft was fixed on the tibial side with an 18 mm extended-spiked WasherLoc.

Immediately following ACL reconstruction, the legs were reinserted into the loading apparatus. Simultaneous radiographs were taken in two planes (*A-P* view and lateral view) of the knee to define an anatomical coordinate system [14,17,18]. Simultaneous radiographs were taken as a 90 N posterior force, 30 N anterior tare force, 150 N anterior force, and 30 N anterior tare force were each transmitted at the knee. The second application of the 30 N anterior tare force was necessary to determine a reference value of the elastic deformation. The reference value was the total deformation at the first 150 N anterior force minus the plastic deformation from the second application of the 30 N anterior tare force (see Appendix). The knees were then cyclically loaded 1500 times at $\frac{1}{4}$ Hz between the 90 N posterior and 150 N anterior forces. This number of loading cycles was chosen because it allows anterior laxity to reach steady state [12]. The cyclic loading was paused after 50 cycles, 120 cycles, 280 cycles, 650 cycles, and 1500 cycles, at which time simultaneous radiographs were taken while the 30 N anterior tare force and 150 N anterior force were transmitted at the knee. These cycle intervals were based on a logarithmic scale so that more measurements would be made during the initial cycles when the greatest increases in lengthening were expected to occur [13]. The 30 N anterior tare force was determined in a pilot study conducted on three specimens and was the minimum shear force transmitted by the knee necessary to create 6 N of graft tension after the graft length had been increased so that the initial graft tension was 0.

To determine empirical relationships between the length of the graft construct and the 30 N anterior tare and 150 N anterior laxities (Objective 2), simultaneous radiographs were taken as the graft construct was lengthened in millimeter increments. After the knee had been cyclically loaded for 1500 cycles, the initial tension was restored by placing the knee in full extension and adjusting the adjustable femoral fixation to restore 110 N to the graft. The graft tension was reset to 110 N to negate plastic deformations that occurred during cyclic loading and hence restore *A-P* laxity to normal [13]. The knee was placed in 25 deg of flexion and the graft construct was lengthened to 7 mm in millimeter increments. Simultaneous radiographs were taken while 30 N anterior tare force and 150 N anterior force were transmitted at the knee and at each millimeter increment in the length of the graft construct.

To determine the increase in the 30 N anterior tare laxity before the graft force reaches zero (Objective 3), the graft force was measured as the 30 N anterior tare force was transmitted at the knee. A load cell was attached to the adjustable femoral fixation device. For each incremental increase in the graft construct length, the force in the load cell was recorded while the 30 N anterior tare force was applied. This force was multiplied by an experimentally determined ratio of 1.16 to correct for friction between the graft and femoral tunnel and hence determine the force in the intraarticular portion of the graft [13].

Data Analysis. Analysis of the radiographs was performed using a customized RSA data analysis system described previously [22]. Briefly, a digital image was obtained for each radiograph using a back-lit scanner (Epson 1600, Epson America Inc., Long Beach, CA). The two-dimensional centroid coordinates of the markers were measured from the digital image using a software program (SCION IMAGE 1.0, Scion Corporation, Frederick, MD). A customized computer program written in MATLAB (Version 6.0, The Mathworks Inc., Natick, MA) was used to determine *A-P* knee laxity and the eight causes of lengthening associated with the tibial and femoral fixations. This program initially computed the transformation of image coordinates to the calibration cage, the positions of the roentgen foci, and the 3D position coordinates of all the markers in a laboratory coordinate system defined by the calibration cage [24]. A center-of-rotation tibial coordinate system was established using anatomical landmarks seen from the *A-P*

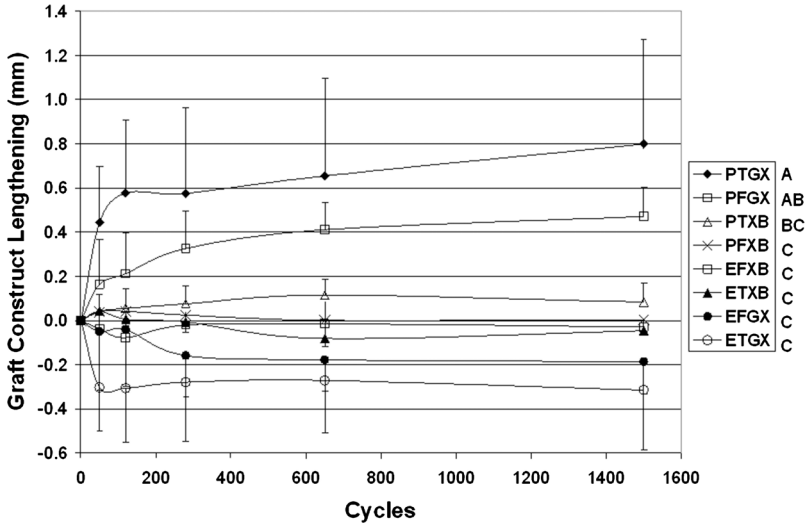

Fig. 5 The eight causes of lengthening of an ACL soft-tissue graft construct associated with the fixations versus the number of load cycles. The four plastic causes are (1) between the femoral fixation and bone (PFXB), (2) between the graft and femoral fixation (PFGX), (3) between the graft and tibial fixation (PTGX), and (4) between the tibial fixation and bone (PTXB). The four elastic causes are lengthening due to a decrease in elastic stiffness (1) between the femoral fixation and bone (EFXB), (2) between the graft and femoral fixation (EFGX), (3) between the graft and tibial fixation (ETGX), and (4) between the tibial fixation and bone (ETXB). Negative values indicate shortening. The standard deviations are shown. Causes with the same letter were not statistically different (α=0.05).

and lateral radiographs with the leg in the unloaded position [17]. The origin was the intersection of the line passing through the centers of the posterior femoral condyles and the line that bisects the femur in the coronal plane. The anterior direction (+x-axis) of the anatomical coordinate system was defined from the line formed by markers implanted in the housing of the pneumatic actuator. The distal direction (+z-axis) was the cross product of x and the line passing through the centers of the posterior femoral condyles. The lateral direction (+y-axis) was the cross product of z and x. *A-P* knee laxity for the 30 N anterior tare force and 150 N anterior force transmitted at the knee was determined by computing the relative motion between the tibia and femur along the x-axis.

The eight causes of lengthening associated with the fixations were computed according to the equations in the Appendix (Objective 1). A single-factor ANOVA was used to determine whether there were differences in lengthening due to the eight causes after 1500 loading cycles. The independent variable was the cause at eight levels and the dependent variable was the amount of lengthening due to each cause. A Tukey's test was used to determine which cause(s) was significantly greatest. For all statistical analyses, the level of significance was set to α=0.05.

To determine whether an empirical relationship can be used to predict the two causes associated with the graft (Objective 2), the seven incremental increases in graft length were plotted versus the 30 N anterior tare laxity and 150 N anterior laxity values for all specimens. Simple linear regressions were used for the 30 N anterior tare force and 150 N anterior force relationships and the 95% prediction intervals were computed. The random error (i.e., standard deviation) associated with the intervals was used as a measure of the error in predicting an increase in the graft construct length for a given increase in the 30 N anterior tare and 150 N anterior laxities.

To determine how much the 30 N anterior tare laxity can increase before the graft force reaches zero (Objective 3), the 30 N anterior tare laxity was computed for each incremental increase in the length of the graft construct. Due to a 6 N uncertainty in predicting the weight of the shank and foot, 6 N of graft force was used to establish a threshold for the maximum allowable increase in the 30 N anterior tare laxity. When the threshold is reached, the lengthening due to the plastic and elastic causes cannot be differentiated.

Results

The increase in anterior laxity at 150 N of force transmitted by the knee was 2.5 ± 1.5 mm after 1500 loading cycles. Of the eight causes associated with the fixations, the greatest after 1500 loading cycles was plastic deformation between the graft and tibial fixation (0.8 mm mean $\pm$0.5 mm standard deviation) followed by the plastic deformation between the graft and femoral fixation (0.5 ± 0.1 mm) (Fig. 5). However, these two causes were not significantly different ($p > 0.05$). The change in elastic stiffness between the graft and tibial fixation and between the graft and femoral fixation led to shortenings of the graft construct of 0.3 ± 0.3 mm and 0.2 ± 0.1 mm, respectively. This indicates that the stiffness increased as the number of loading cycles increased. The remaining four causes were close to 0.

The empirical relationships between an increase in length of the graft construct and increase in the 30 N anterior tare and 150 N anterior laxities were linear with r-squared values exceeding 0.85 (Figs. 6 and 7). For each millimeter increase in the 30 N anterior tare laxity and 150 N anterior laxity, the graft construct lengthened by 0.8 mm and 1.0 mm, respectively. The random errors in predicting the increase in graft construct length for a given increase in the 30 N anterior tare laxity (plastic cause) and for a given increase in the 150 N anterior laxity (elastic cause) are 0.9 mm and 0.5 mm, respectively.

The minimum increase in the 30 N anterior tare laxity before the graft force reached 6 N was 5.3 mm (Fig. 8).

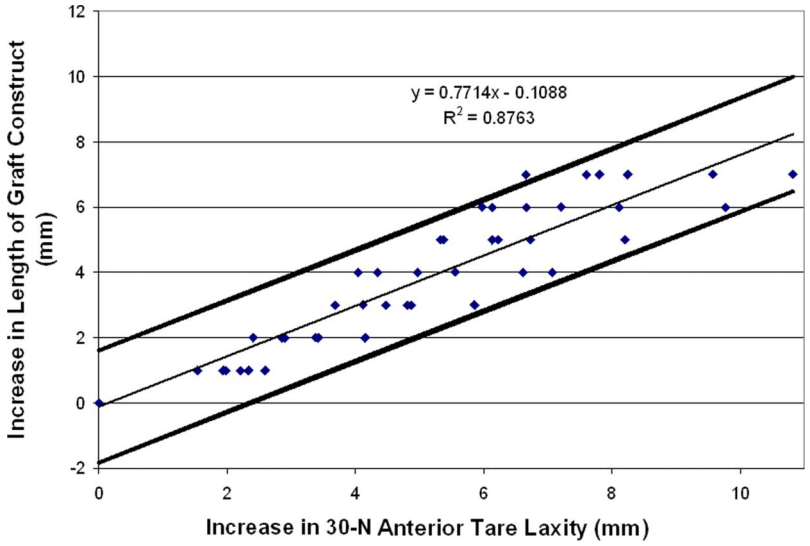

Fig. 6 Empirical relationship between the increase in length of the graft construct and the increase in the 30 N anterior tare laxity. The 95% prediction interval is plotted and is ±1.8 mm. The random error (i.e., 1 standard deviation) in using this relationship to predict the increase in length of the graft construct is 0.9 mm.

Discussion

Because a percentage of the patient population with knees reconstructed with single-loop tibialis tendon allografts do not benefit from a clinically stable knee and because lengthening of the graft construct is the source of a clinically unstable knee, it is of interest to develop a methodology for determining the causes of the increase in the length of a graft construct, which could be used in vivo. Hence, the objectives of our study were (1) to develop the methods to determine the eight causes associated with the fixations using RSA and to demonstrate the usefulness of these methods during cyclic loading of cadaveric knees, (2) to determine an empirical relationship between an increase in length of the graft construct and an increase in anterior laxity using RSA and assess whether this relationship can be used to predict the two causes associated with the graft, and (3) to determine the increase in the 30 N anterior tare laxity before the graft force is zero under a 30 N anterior tare force. Our key findings are that the eight causes associated with the fixations of an increase in anterior laxity can be determined using RSA, provided that the increase in the 30 N anterior tare laxity is less than 5 mm. The remaining two causes associated with the graft (i.e., plastic deformation and lengthening due to elastic stiffness changes) can be determined with quantified random errors using empirical relationships.

There are two potential sources of error associated with our RSA analysis: the inherent error associated with the RSA system and the migration of markers in the tendon graft under cyclic load. The inherent error associated with the RSA system is 0.05 mm [22], while the migration of markers injected into single-looped grafts is 0.10 mm [23]. Only the inherent error would affect the four causes between the fixations and bones, while the migration

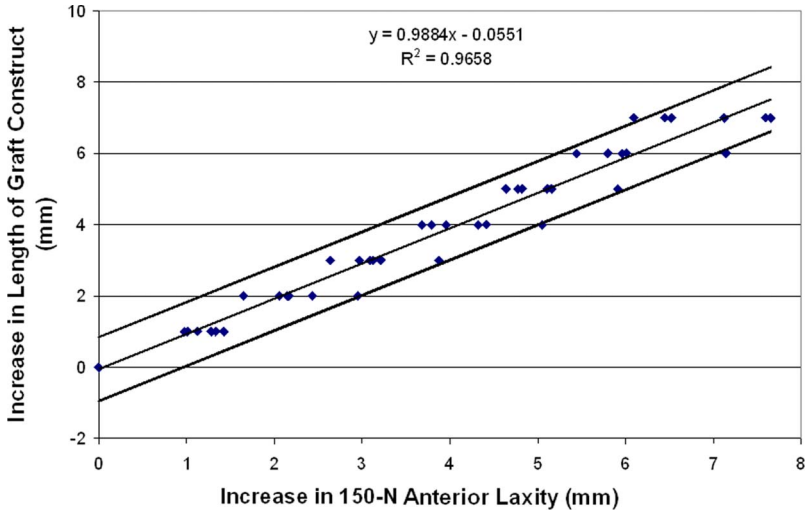

Fig. 7 Empirical relationship between the increase in length of the graft construct and increases in the 150 N anterior laxity. The 95% prediction interval is plotted and is ±0.9 mm. The random error (i.e., 1 standard deviation) in using this relationship to predict the increase in length of the graft construct is 0.5 mm.

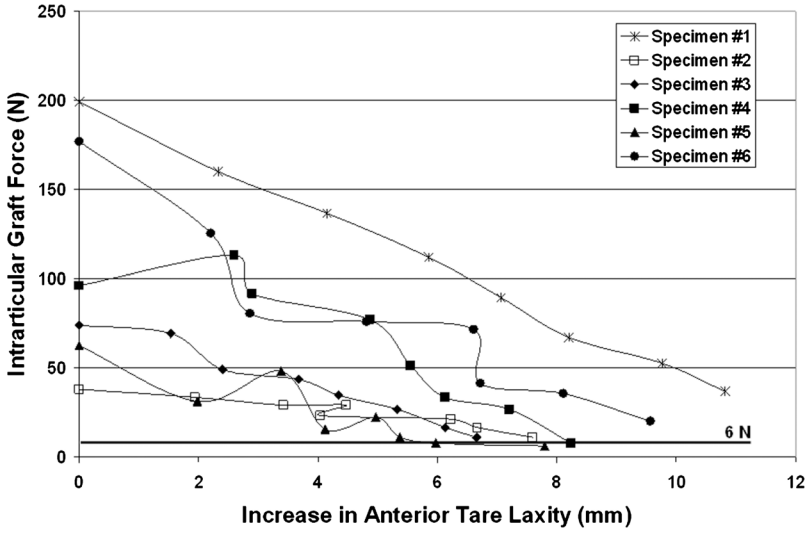

Fig. 8 Plot showing the increase in anterior tare laxity versus the intra-articular graft force. The minimum increase in anterior tare laxity before the graft force reaches 6 N is 5.3 mm.

error would affect the remaining four causes between the graft and fixations. In either case, these sources of error are small in relation to the 3 mm of lengthening considered clinically important [25,26] so that high confidence can be placed in the amounts of the various causes, which contribute substantively to lengthening of the graft construct.

Of the eight causes associated with the fixations, the greatest after 1500 loading cycles was plastic deformation between the graft and tibial fixation (0.8 mm on average). However, the total lengthening at the site of tibial fixation was less because there was a decrease in lengthening (0.3 mm on average) caused by an increase in elastic stiffness between the graft and tibial fixation. Hence, the total lengthening associated with the tibial fixation device was 0.5 mm on average. Nevertheless, the plastic deformation between the graft and tibial fixation is still undesirable, particularly because it would likely occur in vivo as well as in vitro; the small number of loading cycles applied in our in vitro study would quickly be reached in vivo following ACL reconstruction. Hence, it is useful to consider means of decreasing this deformation. Possibilities include either using a secondary fixation in series [27] or modifying the fixation device so that the fixation to the graft is improved. For example, for the WasherLoc (Fig. 4), this device might be modified by adding more spikes, increasing the diameter of the spikes, changing the cross-sectional shape of the spikes, and changing the pattern of the spikes.

The second greatest cause of an increase in anterior laxity was plastic deformation between the graft and femoral fixation (0.5 mm on average). Plastic deformation between the graft and femoral fixation has been observed previously and results from water being expelled from the tendon as it is deformed around the pin, which supports the graft (Fig. 4) [6]. Considering this mechanism, preoperative treatment of the graft could be used to minimize this cause. This treatment might include looping the graft around a pin while applying a tensile load and allowing the graft to expel the water while monitoring the temperature and the tension applied to the graft prior to insertion into the tunnels [28].

Although the lengthening due to plastic deformation between the femoral fixation and bone and change in elastic stiffness between the femoral fixation and bone was near zero (Fig. 5), these results may not be clinically represented. This is because the femoral fixation device used in our study was custom made, which was necessitated by the need to change the length of the graft construct to address our third objective. To secure our custom femoral fixation device to the femur, a mantle of bone cement on the cortex of the femur was required. Although no femoral fixation device is known to the authors, which is used clinically and relies on such a method of support, the EZLoc femoral fixation device, which is in common use clinically, also rests on the femoral cortex. Because of the hardness of the femoral cortex, minimal relative motion between the bone and fixation is expected for both our custom device and the clinical device so that our results for these two causes may apply to the EZLoc but this remains to be demonstrated.

To determine the plastic deformation and lengthening caused by a change in the elastic stiffness of the graft using RSA, two methods are available. One method is to inject multiple markers spaced along the intrarticular space of the graft and monitor how their positions change over time. This was done previously in double-looped and patellar tendon grafts and it was shown that the markers in the intrarticular space migrated in the graft while the graft markers in the locations of the tunnels did not migrate in the graft [9]. Because it is possible that the markers might migrate from the tendon to the intrarticular space and become a loose body in the knee joint, we chose to evaluate the second method, which is to determine the deformations of the graft based on regression equations. If the eight causes associated with the fixations are known and if the relationships between the increase in length of the graft construct and increases in the 30 N anterior tare and 150 N anterior laxities are known, then the deformations of the graft can be computed (Eqs. (A5) and (A14) in the Appendix). However, there were random errors in predicting the increase in graft construct length for a given increase in the 30 N anterior tare and 150 N anterior laxity of 0.9 mm and 0.5 mm, respectively. To put these errors into perspective, a 3 mm increase in anterior laxity is a threshold of instability in a reconstructed knee [25,26]. Hence, if these empirical relationships are used, then these two causes will be prone to random errors of 30% and 17%, which are substantial.

Our millimeter-for-millimeter relationship between increases in graft construct length and increases in the 150 N anterior laxity using RSA (Fig. 7) agrees with previous research, which determined this relationship using an arthrometer [10,11]. The anterior laxity determined using an arthrometer rarely correlates well with the anterior laxity determined using RSA [29–32]. This is expected because anterior laxity measurements using RSA and arthrometers depend on many factors [16,17,25,33]. Yet, our study agrees with multiple studies, which used different methods for determining anterior laxity. This is because only the increases in anterior laxity and not the laxity values themselves were exam-

ined in our study. Another study showed similar increases in anterior laxity determined using RSA and an arthrometer [14]. Therefore, we conclude that the anterior laxity is method dependent, whereas the increase in anterior laxity is not.

To differentiate between the plastic deformations and increases in elastic deformations, application of a tare force to the tibia that will apply a small tensile force to the graft is required. However, if the graft is not taut, then the plastic deformations will be prone to error. Because the graft force cannot be measured in vivo, it was necessary to relate the graft force to anterior tare laxity in our in vitro study. The minimum increase in the 30 N anterior tare laxity that caused the graft force to decrease to 6 N was 5 mm. The 6 N value was chosen instead of zero because 6 N is the error in determining the mass of the shank and foot [15]. Hence, if the 30 N anterior tare laxity increases more than 5 mm, then the plastic and elastic causes cannot be differentiated.

Nevertheless, the causes associated with the fixations can still be determined, but they will be a combination of the plastic and elastic causes (e.g., plastic deformation between the graft and tibial fixation (PTGX) and increase in elastic deformation between the graft and tibial fixation (ETGX) will be CTGX, where the C stands for combined). The combined results have been published previously for doubled-looped semitendinosus and gracilis and patellar tendon grafts with interference screws [9]. The combined results can still be used to identify the causes of an increase in the 150 N anterior laxity; however, these results will not provide the same level of detail in identifying the causes.

While our methods distinguish and determine eight causes of lengthening associated with the fixations as long as the increase in the 30 N anterior laxity is less than 5 mm, our methods do not separately measure every possible cause of lengthening. Among the eight causes associated with the fixations are plastic deformation between the fixation and bone and increases in elastic deformation between the fixation and bone. Contributing to either cause is deformation of the bone at the bone-fixation interface and deformation of the fixation device per se, which could be considered conceptually as two different causes. With this conceptual distinction, the total number of causes would increase from 10 to 14. However, it is difficult to separately measure deformations of both the bone and fixation device using conventional RSA, which requires that markers be attached to points of interest. When the deformation between the fixation and bone is determined using our methods, the sum of the bone deformation and deformation of the fixation device is reflected. For those fixations that demonstrate relatively large amounts of lengthening between the fixation and bone, it might be worthwhile to focus future efforts on developing RSA methods to determine deformation of the bone(s) separately from that of the fixation(s).

In summary, we have shown that RSA is a useful tool for determining eight causes associated with the fixations of lengthening of a soft-tissue ACL graft construct, provided that the 30 N anterior tare laxity increases less than 5 mm. With increases in the 30 N anterior tare laxity greater than 5 mm, the causes associated with the fixations can still be determined but the plastic causes cannot be differentiated from the elastic causes. The remaining two causes associated with the graft can be predicted using the regression models presented herein with defined random errors that are large.

Acknowledgment

The authors would like to thank the Musculoskeletal Transplant Foundation for support of this research project.

Appendix: Equations to Compute the Causes of Lengthening of an Anterior Cruciate Ligament Graft

The deformation between the graft and tibial fixation was determined using the two tendon markers placed closest to the WasherLoc (G1, G8, and WL, Fig. 3). Initially and after cyclic loading, the position vectors $\mathbf{P}^{G1/WL}$ and $\mathbf{P}^{G8/WL}$ locating the tendon markers from the WasherLoc marker were computed. The amount of deformation in the tibia between the graft and the fixation (TGX) was determined as the average vector change of $\mathbf{P}^{G1/WL}$ and $\mathbf{P}^{G8/WL}$ projected along the axis of the tibial tunnel by the equation

$$\mathrm{TGX} = \frac{\Delta\mathbf{P}^{G1/WL} \cdot \mathbf{T} + \Delta\mathbf{P}^{G8/WL} \cdot \mathbf{T}}{2|\mathbf{T}|} \tag{A1}$$

where $\Delta\mathbf{P}^{G1/WL}$ and $\Delta\mathbf{P}^{G8/WL}$ are the vector differences (final minus initial) of the vector to G1 from WL and the vector to G8 from WL, respectively, while $\mathbf{T}$ is the vector along the axis of the tibial tunnel.

The deformation between the graft and the femoral fixation was determined using the two tendon markers placed closest to the adjustable femoral fixation device (G4, G5, and EL, Fig. 3). Initially and after cyclic loading, the vectors $\mathbf{P}^{G4/EL}$ and $\mathbf{P}^{G5/EL}$ locating the tendon markers from the adjustable femoral fixation device marker were computed. The amount of deformation in the femur between the graft and the fixation (FGX) was determined as the average vector change of $\mathbf{P}^{G4/EL}$ and $\mathbf{P}^{G5/EL}$, projected along the axis of the femoral tunnel by the equation

$$\mathrm{FGX} = \frac{\Delta\mathbf{P}^{G4/EL} \cdot \mathbf{F} + \Delta\mathbf{P}^{G5/EL} \cdot \mathbf{F}}{2|\mathbf{F}|} \tag{A2}$$

where $\Delta\mathbf{P}^{G4/EL}$ and $\Delta\mathbf{P}^{G5/EL}$ are the vector differences (final minus initial) of the vector to G4 from EL and to G5 from EL, respectively, while $\mathbf{F}$ is the vector along the axis of the femoral tunnel.

The deformation between the tibial fixation and bone was determined using the marker welded to the WasherLoc and marker T1 (WL and T1, Fig. 3). Initially and after cyclic loading, the position vector $\mathbf{P}^{T1/WL}$ locating the WasherLoc from the tibia was computed. The amount of deformation between the tibial fixation and bone (TXB) was determined as the vector change of $\mathbf{P}^{T1/WL}$ from the initial vector, projected along the axis of the tibial tunnel by the equation

$$\mathrm{TXB} = \frac{\Delta\mathbf{P}^{T1/WL} \cdot \mathbf{T}}{|\mathbf{T}|} \tag{A3}$$

where $\Delta\mathbf{P}^{T1/WL}$ is the vector difference (final minus initial) of the vector to T1 from WL.

The deformation between the femoral fixation and bone was determined using the tendon marker welded to the adjustable femoral fixation device and marker F1 on the femur (EL and F1, Fig. 3). Initially and after cyclic loading, the position vector $\mathbf{P}^{F1/EL}$ locating the adjustable femoral fixation device from the femur was computed. The amount of deformation between the femoral fixation and bone (FXB) was determined as the vector change of $\mathbf{P}^{F1/EL}$ from the initial vector, projected along the axis of the femoral tunnel by the equation

$$\mathrm{FXB} = \frac{\Delta\mathbf{P}^{F1/EL} \cdot \mathbf{F}}{|\mathbf{F}|} \tag{A4}$$

where $\Delta\mathbf{P}^{F1/EL}$ is the vector difference (final minus initial) of the vector to F1 from EL.

The amount of plastic deformation corresponding to each of the four causes associated with the fixations was computed according to Eqs. (A1)–(A4) where the final vector lengths were computed for the 30 N anterior tare force transmitted at the knee and the initial vector lengths were computed for the first application of the 30 N anterior tare force transmitted at the knee. These plastic deformations are denoted by PTGX and PTXB for the tibial fixation and PFGX and PFXB for the femoral fixation. The plastic deformation of the graft substance between the fixations was determined indirectly. The amount of plastic lengthening of the graft substance between the fixations (PG) was calculated as

$$PG = K_1 \Delta L_{30} - (PFGX + PFXB) - (PTGX + PTXB) \quad (A5)$$

where ΔL_{30} is the change in the 30 N anterior tare laxity with respect to the first application of the 30 N anterior tare force transmitted at the knee and K_1 is the slope from the relationship between the length of the graft construct and 30 N anterior tare laxity. Note that in all of the above computations for plastic lengthening of a graft construct, both the initial vector and the final vector were determined for the 30 N anterior tare force transmitted at the knee.

To compute the lengthening of the graft construct due to changes in stiffness, the elastic deformation was computed for the first load cycle. Equations (A1)–(A4) were used to compute the total elastic deformation for each fixation except that the final vector lengths were computed for the 150 N anterior force and the initial vector lengths were computed for the second application of the 30 N anterior tare force. The lengthening of the graft construct due to the initial stiffness of the femoral fixation components for the first application of the 150 N anterior force is given by

$$EFXB_i = FXB_{150} \quad (A6)$$

$$EFGX_i = FGX_{150} \quad (A7)$$

where FXB_{150} and FGX_{150} are the two elastic deformations at the femoral site of fixation. Similarly, the lengthening of the graft construct due to the initial stiffness of the tibial fixation components is given by

$$ETXB_i = TXB_{150} \quad (A8)$$

$$ETGX_i = TGX_{150} \quad (A9)$$

where TXB_{150} and TGX_{150} are the two elastic deformations at the tibial site of fixation.

The lengthening of the graft construct due to changes in stiffness of the femoral and tibial fixations was computed as

$$EFXB = FXB_{150} - EFXB_i - PFXB \quad (A10)$$

$$EFGX = FGX_{150} - EFGX_i - PFGX \quad (A11)$$

$$ETXB = TXB_{150} - ETXB_i - PTXB \quad (A12)$$

$$ETGX = TGX_{150} - ETGX_i - PTGX \quad (A13)$$

The lengthening of the graft construct due to changes in the stiffness of the graft (EG) was computed as

$$EG = K_2 \Delta L_{150} - EFXB - EFGX - ETXB - ETGX - K_1 \Delta L_{30} \quad (A14)$$

where ΔL_{150} is the change in the 150 N anterior laxity with respect to the first application of the 150 N anterior force transmitted at the knee, ΔL_{30} is the change in the 30 N anterior tare laxity with respect to the first application of the 30 N anterior tare force transmitted at the knee, and K_2 is the slope value from the relationship between the length of the graft construct and the 150 N anterior laxity.

References

[1] Nyland, J., Caborn, D. N., Rothbauer, J., Kocabey, Y., and Couch, J., 2003, "Two-Year Outcomes Following ACL Reconstruction With Allograft Tibialis Anterior Tendons: A Retrospective Study," Knee Surg. Sports Traumatol. Arthrosc, **11**(4), pp. 212–218.

[2] Caborn, D. N., and Selby, J. B., 2002, "Allograft Anterior Tibialis Tendon With Bioabsorbable Interference Screw Fixation in Anterior Cruciate Ligament Reconstruction," Arthroscopy: J. Relat. Surg., **18**(1), pp. 102–105.

[3] Chang, S. K., Egami, D. K., Shaieb, M. D., Kan, D. M., and Richardson, A. B., 2003, "Anterior Cruciate Ligament Reconstruction: Allograft Versus Autograft," Arthroscopy: J. Relat. Surg., **19**(5), pp. 453–462.

[4] Pearsall, A. W., Hollis, J. M., Russell, G. V., Jr., and Scheer, Z., 2003, "A Biomechanical Comparison of Three Lower Extremity Tendons for Ligamentous Reconstruction About the Knee," Arthroscopy: J. Relat. Surg., **19**(10), pp. 1091–1096.

[5] Haut Donahue, T. L., Howell, S. M., Hull, M. L., and Gregersen, C., 2002, "A Biomechanical Evaluation of Anterior and Posterior Tibialis Tendons as Suitable Single-Loop Anterior Cruciate Ligament Grafts," Arthroscopy: J. Relat. Surg., **18**(6), pp. 589–597.

[6] Roos, P. J., Hull, M. L., and Howell, S. M., 2004, "Lengthening of Double-Looped Tendon Graft Constructs in Three Regions After Cyclic Loading: A Study Using Roentgen Stereophotogrammetric Analysis," J. Orthop. Res., **22**(4), pp. 839–846.

[7] Adam, F., Pape, D., Schiel, K., Steimer, O., Kohn, D., and Rupp, S., 2004, "Biomechanical Properties of Patellar and Hamstring Graft Tibial Fixation Techniques in Anterior Cruciate Ligament Reconstruction: Experimental Study With Roentgen Stereometric Analysis," Am. J. Sports Med., **32**(1), pp. 71–78.

[8] Smith, C. K., Hull, M. L., and Howell, S. M., 2006, "Lengthening of a Single-Loop Tibialis Tendon Graft Construct After Cyclic Loading: A Study Using Roentgen Stereophotogrammetric Analysis," J. Biomech. Eng., **128**(3), pp. 437–442.

[9] Khan, R., Konyves, A., Rama, K. R., Thomas, R., and Amis, A. A., 2006, "RSA Can Measure ACL Graft Stretching and Migration: Development of a New Method," Clin. Orthop. Relat. Res., **448**, pp. 139–145.

[10] Cuppone, M., and Seedhom, B. B., 2001, "Effect of Implant Lengthening and Mode of Fixation on Knee Laxity After ACL Reconstruction With an Artificial Ligament: A Cadaveric Study," J. Orthop. Sci., **6**(3), pp. 253–261.

[11] Grover, D., Thompson, D., Hull, M. L., and Howell, S. M., 2006, "Empirical Relationship Between Lengthening an Anterior Cruciate Ligament Graft and Increases in Knee Anterior Laxity: A Human Cadaveric Study," J. Biomech. Eng., **128**(6), pp. 969–972.

[12] Arnold, M. P., Lie, D. T., Verdonschot, N., de Graaf, R., Amis, A. A., and van Kampen, A., 2005, "The Remains of Anterior Cruciate Ligament Graft Tension After Cyclic Knee Motion," Am. J. Sports Med., **33**(4), pp. 536–542.

[13] Grover, D. M., Howell, S. M., and Hull, M. L., 2005, "Early Tension Loss in an Anterior Cruciate Ligament Graft. A Cadaver Study of Four Tibial Fixation Devices," J. Bone Jt. Surg., Am. Vol., **87**(2), pp. 381–390.

[14] Fleming, B. C., Brattbakk, B., Peura, G. D., Badger, G. J., and Beynnon, B. D., 2002, "Measurement of Anterior-Posterior Knee Laxity: A Comparison of Three Techniques," J. Orthop. Res., **20**(3), pp. 421–426.

[15] Zatsiorsky, V. M., 2002, *Kinetics of Human Motion*, Human Kinetics, Champaign, IL, pp. 653.

[16] Markolf, K. L., Burchfield, D. M., Shapiro, M. M., Davis, B. R., Finerman, G. A., and Slauterbeck, J. L., 1996, "Biomechanical Consequences of Replacement of the Anterior Cruciate Ligament With a Patellar Ligament Allograft. Part I: Insertion of the Graft and Anterior-Posterior Testing," J. Bone Jt. Surg., Am. Vol., **78**(11), pp. 1720–1727.

[17] Roos, P. J., Neu, C. P., Hull, M. L., and Howell, S. M., 2005, "A New Tibial Coordinate System Improves the Precision of Anterior-Posterior Knee Laxity Measurements: A Cadaveric Study Using Roentgen Stereophotogrammetric Analysis," J. Orthop. Res., **23**(2), pp. 327–333.

[18] Friden, T., Ryd, L., and Lindstrand, A., 1992, "Laxity and Graft Fixation After Reconstruction of the Anterior Cruciate Ligament. A Roentgen Stereophotogrammetric Analysis of 11 Patients," Acta Orthop. Scand., **63**(1), pp. 80–84.

[19] Bailey, S. B., Grover, D. M., Howell, S. M., and Hull, M. L., 2004, "Foam-Reinforced Elderly Human Tibia Approximates Young Human Tibia Better Than Porcine Tibia: A Study of the Structural Properties of Three Soft Tissue Fixation Devices," Am. J. Sports Med., **32**(3), pp. 755–764.

[20] Simmons, R., Howell, S. M., and Hull, M. L., 2003, "Effect of the Angle of the Femoral and Tibial Tunnels in the Coronal Plane and Incremental Excision of the Posterior Cruciate Ligament on Tension of an Anterior Cruciate Ligament Graft: An in Vitro Study," J. Bone Jt. Surg., Am. Vol., **85-A**,(6), pp. 1018–1029.

[21] Howell, S. M., Gittens, M. E., Gottlieb, J. E., Traina, S. M., and Zoellner, T. M., 2001, "The Relationship Between the Angle of the Tibial Tunnel in the Coronal Plane and Loss of Flexion and Anterior Lexity After Anterior Cruciate Ligament Reconstruction," Am. J. Sports Med., **29**(5), pp. 567–574.

[22] Roos, P. J., Hull, M. L., and Howell, S. M., 2004, "How Cyclic Loading Affects the Migration of Radio-Opaque Markers Attached to Tendon Grafts Using a New Method: A Study Using Roentgen Stereophotogrammetric Analysis (RSA)," J. Biomech. Eng., **126**(1), pp. 62–69.

[23] Smith, C. K., Hull, M. L., and Howell, S. M., 2005, "Migration of Radio-Opaque Markers Injected Into Tendon Grafts: A Study Using Roentgen Stereophotogrammetric Analysis (RSA)," J. Biomech. Eng., **127**(5), pp. 887–890.

[24] Selvik, G., 1989, "Roentgen Stereophotogrammetry. A Method for the Study of the Kinematics of the Skeletal System," Acta Orthop. Scand. Suppl., **232**, pp. 1–51.

[25] Daniel, D. M., Stone, M. L., Sachs, R., and Malcom, L., 1985, "Instrumented Measurement of Anterior Knee Laxity in Patients With Acute Anterior Cruciate Ligament Disruption," Am. J. Sports Med., **13**(6), pp. 401–407.

[26] Steiner, M. E., Brown, C., Zarins, B., Brownstein, B., Koval, P. S., and Stone, P., 1990, "Measurement of Anterior-Posterior Displacement of the Knee. A Comparison of the Results With Instrumented Devices and With Clinical Examination," J. Bone Jt. Surg., Am. Vol., **72**(9), pp. 1307–1315.

[27] Weiler, A., Richter, M., Schmidmaier, G., Kandziora, F., and Sudkamp, N. P., 2001, "The Endopearl Device Increases Fixation Strength and Eliminates Construct Slippage of Hamstring Tendon Grafts With Interference Screw Fixation," Arthroscopy: J. Relat. Surg., **17**(4), pp. 353–359.

[28] Ciccone, W. J., II, Bratton, D. R., Weinstein, D. M., and Elias, J. J., 2006, "Viscoelasticity and Temperature Variations Decrease Tension and Stiffness of Hamstring Tendon Grafts Following Anterior Cruciate Ligament Reconstruction," J. Bone Jt. Surg., Am. Vol., **88**(5), pp. 1071–1078.

[29] Jonsson, H., Karrholm, J., and Elmqvist, L. G., 1993, "Laxity After Cruciate

Ligament Injury in 94 Knees. The KT-1000 Arthrometer Versus Roentgen Stereophotogrammetry," Acta Orthop. Scand., **64**(5), pp. 567–570.
[30] Brandsson, S., Karlsson, J., Sward, L., Kartus, J., Eriksson, B. I., and Karrholm, J., 2002, "Kinematics and Laxity of the Knee Joint After Anterior Cruciate Ligament Reconstruction: Pre- and Postoperative Radiostereometric Studies," Am. J. Sports Med., **30**(3), pp. 361–367.
[31] Friden, T., Sommerlath, K., Egund, N., Gillquist, J., Ryd, L., and Lindstrand, A., 1992, "Instability After Anterior Cruciate Ligament Rupture. Measurements of Sagittal Laxity Compared in 11 Cases," Acta Orthop. Scand., **63**(6), pp. 593–598.
[32] Jorn, L. P., Friden, T., Ryd, L., and Lindstrand, A., 1998, "Simultaneous Measurements of Sagittal Knee Laxity With an External Device and Radiostereometric Analysis," J. Bone Joint Surg. Br., **80**(1), pp. 169–172.
[33] Fleming, B. C., Beynnon, B. D., and Johnson, R. J., 1993, "The Use of Knee Laxity Testers for the Determination of Anterior-Posterior Stability of the Knee: Pitfalls in Practice.," in *The Anterior Cruciate Ligament: Current and Future Concepts*, D. Jackson, ed., Raven, New York, pp. 239–250.